ISSN 1738-8716(Print)
ISSN 2287-8130(Online)
Particle and Aerosol Research
Part. Aerosol Res. Vol. 14, No. 1: March 2018 pp. 1-8
http://dx.doi.org/10.11629/jpaar.2018.14.1.001

Analytical approximation of optical force on a perfectly reflecting sphere: ray-optics regime

Sang Bok Kim · Dong Keun Song[1)]

[1)]*Department of Environmental Machinery, Environment System Research Division*
Korea Institute of Machinery and Materials,
156 Gajeongbuk-ro, Yuseong-gu, Daejeon, 34103, Republic of Korea

(Received 16 March 2018; Revised 22 March 2018; Accepted 23 March 2018)

Abstract

The optical force on a perfectly reflecting sphere in a ray-optics regime is considered. With the assumption of geometric optics and a sphere smaller than the minimum waist of the illuminating beam, closed-form analytic expressions of the optical force are derived. Both axial and radial forces are expressed by a modified Bessel function of the first kind. The derived analytic expressions are compared to precise numerical computations of the exact optical force equations derived previously. In addition the error due to the small sphere assumption is estimated analytically.

Keywords: Optical force; Perfectly reflecting sphere; Sonine integral; Bessel function.

* Corresponding author.
Tel : +82-42-868-7271, Fax : +82-42-868-7284
E-mail : dksong@kimm.re.kr

1. Introduction

The existence of the radiation pressure force, or optical force, from the Sun was predicted by Kepler based on his observation of comet tails in the early 17th century. Due to the lack of a proper light source, however, the optical force was not able to be verified experimentally until the development of the laser. Ashkin's demonstration of the acceleration and levitation of micron-sized objects using a laser beam in the early 1970s initiated the use of optical force in diverse fields of research including physics (Ashkin, 1970; Chu et al., 1986; Ozornek et al., 1998), biology (Ashkin and Dziedzic, 1989; Finer et al., 1994; Hebert et al., 2011; Paik and Perkins, 2012; Zhong et al., 2013), and engineering (Gauthier, 1997; Koehler, 1997; Kovac and Voldman, 2007).

Numerous theoretical approaches to optical force have been developed. Principally, it can be computed using the generalized Lorenz-Mie theory for any size of object but it is computationally expensive (Lock, 2004). For two extreme cases, however, computationally efficient methods are available. One is an object much larger than the wavelength of the illuminating beam. In this case the optical force can be obtained in an analytic form using a ray-optics model. The other is an object much smaller than the wavelength of the illuminating beam. In this case dipole approximation can be used. Most of the theoretical studies regarding optical force have focused on transparent dielectric materials including biological cells and polymer spheres. More recently, studies of the optical trapping of absorbing objects have also been reported (Lin and Li, 2014; Pan et al., 2012). In addition, the optical force on a perfectly reflecting sphere has been studied (Kim and Kim, 2006).

Compared to a dielectric object, the optical force on a perfectly reflecting object can take a simpler form because it is not required to account for the infinite paths of rays passing through objects. In a previous study (Kim and Kim, 2006), numerical calculations of optical force on a perfectly reflecting sphere were performed using an approximated expression of the force. An analytic expression of optical force on a perfectly reflecting sphere was also derived but was restricted to a specific spatial coordinate, i.e., the axial force equation was derived for the sphere located along the beam axis (zero radial offset) and the radial force equation was derived for the sphere placed at zero axial distance.

In this study, we derived closed-form expressions of both axial and radial forces on a perfectly reflecting sphere placed at an arbitrary position in the Gaussian beam. We considered a sphere much larger than the wavelength of the illuminating beam, and therefore adopted the ray-optics approach to derive an analytic expression for optical force. Furthermore, we assumed the sphere was smaller than the minimum beam waist that is commonly adopted in optical sorting (Hart et al., 2007; Kaneta et al., 1997; Kim et al., 2006; Kim et al., 2008; Terray et al., 2005; Terray et al., 2009; Terray et al., 2014).

2. Theory

On the assumption of ray-optics, light can be thought of as bundles of rays with zero thickness. The rays change their paths at the interface of the object and surrounding medium due to Snell's law. Because each ray carries momentum, the optical force can be calculated by considering the trajectories of rays passing through an object. Gauthier and Wallace derived the photon stream method to include the effects of the intensity distribution and thereby obtain a closure form of optical force equation (Gauthier and Wallace, 1995). The photon stream path is identical to the trajectory of the ray, and the number of photons in the stream can be calculated from the intensity profile. Therefore, the optical force can be evaluated accurately by considering the change in momentum of all photons passing through an object. Gauthier and Wallace considered only a finite number of photon stream paths, however the photon stream is divided infinitely

whenever it intersects the surface of a sphere. Kim and Kim considered infinite paths of the photon stream and derived an expression for the optical force on a transparent sphere in a loosely focused Gaussian beam (Kim and Kim, 2006),

$$F_a = \frac{n_0}{2c}\int_0^{2\pi}\int_0^{\pi/2} I(\rho,z) \times\left[1+R\cos 2\theta - T^2\frac{\cos 2(\theta-\theta_r)+R\cos 2\theta}{1+R^2+2R\cos 2\theta_r}\right], \times r_p^2 \sin 2\theta \, d\theta d\varphi \quad (1)$$

$$F_r = -\frac{n_0}{2c}\int_0^{2\pi}\int_0^{\pi/2} I(\rho,z) \times\left[R\sin 2\theta - T^2\frac{\sin 2(\theta-\theta_r)+R\sin 2\theta}{1+R^2+2R\cos 2\theta_r}\right], \times r_p^2 \sin 2\theta\cos\varphi \, d\theta d\varphi \quad (2)$$

where F_a and F_r represent the optical force in the axial and negative radial directions, respectively; n_0 is the refractive index of the medium; c is the speed of light in a vacuum; P is the power of the beam; θ and θ_r are the incident and refracted angles of the photon stream at the surface of the sphere; and φ is the polar angle. $I(\rho,z)$ is the Gaussian intensity profile (Saleh and Teich, 2007),

$$I(\rho,z) = \frac{2P}{\pi\omega(z)^2}\exp\left(-\frac{2\rho^2}{\omega(z)^2}\right), \quad (3)$$

where $\omega(z)$ is the radius of the beam at an axial distance z and can be expressed as a function of the minimum beam waist radius, ω_0, and the wavelength of the beam (Saleh and Teich, 2007),

$$\omega(z) = \omega_0\left[1+\left(\frac{\lambda z}{\pi\omega_0^2}\right)^2\right]^{1/2}, \quad (4)$$

and ρ is the radial distance between the ray striking the sphere and the beam center axis and can be expressed as a function of the incident angle and the radial offset of the sphere (Fig. 1),

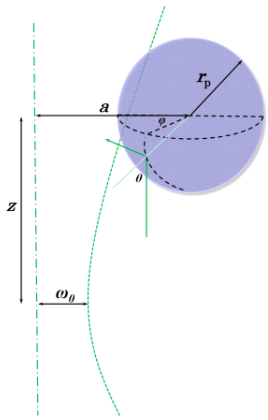

Fig. 1. Geometry considered in this study. The perfectly reflecting sphere is located in the illuminating beam at an arbitrary position.

$$\rho^2 = a^2 + r_p^2\sin^2\theta - 2ar_p\sin\theta\cos\varphi. \quad (5)$$

A loosely focused Gaussian beam was assumed in the derivation of Eqs. (1) and (2), i.e., the minimum beam waist is larger than the wavelength of the illuminating beam. Thus, the photo stream can be thought of as traveling parallel to the direction of propagation and therefore the wavefront radius of curvature can be ignored.

For a perfectly reflecting sphere we can set R = 1 and T = 0 and Eqs. (1) and (2) can be rewritten as,

$$F_{a,exact} = \frac{n_0 P}{\pi c\omega^2}r_p^2\int_0^{2\pi}\int_0^{\pi/2} \exp\left[-2\left(a^2+r_p^2\sin^2\theta - 2ar_p\sin\theta\cos\varphi\right)/\omega^2\right], \times(1+\cos 2\theta)\sin 2\theta \, d\theta \, d\varphi \quad (6)$$

$$F_{r,exact} = -\frac{n_0 P}{\pi c\omega^2}r_p^2\int_0^{2\pi}\int_0^{\pi/2} \exp\left[-2\left(a^2+r_p^2\sin^2\theta - 2ar_p\sin\theta\cos\varphi\right)/\omega^2\right], \times(1+\cos 2\theta)\sin^2 2\theta\cos\varphi \, d\theta \, d\varphi \quad (7)$$

With a small sphere assumption, r_p / ω_0 << 1, and the integral representation of the modified Bessel function of the first kind (Watson, 1995),

$$\mathrm{I}_n(z)=\frac{1}{2\pi}\int_0^{2\pi}\exp(z\cos\varphi)\cos n\varphi\,\mathrm{d}\varphi. \tag{8}$$

Eqs. (6) and (7) can be reduced to single integral forms,

$$F_a=\frac{8n_0P}{c\omega^2}r_\mathrm{p}^2\exp\left(-\frac{2a^2}{\omega^2}\right)\times\int_0^{\pi/2}\mathrm{I}_0\left(\frac{4ar_\mathrm{p}\sin\theta}{\omega^2}\right)\sin\theta\cos^3\theta\,d\theta, \tag{9}$$

$$F_r=-\frac{2n_0P}{c\omega^2}r_\mathrm{p}^2\exp\left(-\frac{2a^2}{\omega^2}\right)\times\int_0^{\pi/2}\mathrm{I}_1\left(\frac{4ar_\mathrm{p}\sin\theta}{\omega^2}\right)\sin^2 2\theta\,d\theta. \tag{10}$$

To calculate the above integral equation, Sonine's integral formula can be applied. The original formulation of Sonine's integral involves a Bessel function of the first kind, $\mathrm{J}_\nu(z)$, but it can be modified as the following (Watson, 1995),

$$\int_0^{\pi/2}\mathrm{I}_\mu(z\sin\theta)\sin^{\mu+1}\theta\cos^{2\nu+1}\theta\,\mathrm{d}\theta=2^\nu\Gamma(\nu+1)z^{-\nu-1}\mathrm{I}_{\mu+\nu+1}(z), \tag{11}$$

with the definition of the modified Bessel function

$$\mathrm{I}_\nu(z)=\exp(-i\pi\nu/2)\mathrm{J}_\nu[z\exp(i\pi/2)]. \tag{12}$$

Here, Γ denotes the gamma function. Finally, the integral form of the axial and radial optical forces can be solved by imposing $\mu = 0$, $\nu = 1$ and $\mu = 1$, $\nu = 1/2$, respectively,

$$F_\mathrm{a,analytic}=\frac{n_0P}{c}\frac{\omega^2}{a^2}\exp\left(-\frac{2a^2}{\omega^2}\right)\mathrm{I}_2\left(\frac{4ar_\mathrm{p}}{\omega^2}\right), \tag{13}$$

$$F_\mathrm{r,analytic}=-\frac{n_0P}{c}\frac{\omega}{a}\sqrt{\frac{\pi r_\mathrm{p}}{2a}}\exp\left(-\frac{2a^2}{\omega^2}\right)\mathrm{I}_{5/2}\left(\frac{4ar_\mathrm{p}}{\omega^2}\right). \tag{14}$$

When the sphere is located at the beam center axis, $a = 0$, Eqs. (13) and (14) become,

$$\lim_{a\to0}F_\mathrm{a,analytic}=\frac{2n_0P}{c}\frac{r_\mathrm{p}^2}{\omega^2}, \tag{15}$$

$$\lim_{a\to0}F_\mathrm{r,analytic}=0, \tag{16}$$

which are identical to equations that can be derived via the direct integration of Eqs. (1) and (2) with $R = 1$ and $T = 0$.

3. Numerical results

To analyze optical force on a perfectly reflecting sphere, numerical calculations were performed and the analytical approximations were compared to the results of the numerical integrations. All length parameters and the optical force were non-dimensionalized by the minimum beam waist radius, ω_0, and momentum flux, n_0P/c, respectively. For all calculations, $\omega_0 = 20\,\lambda$, $r_\mathrm{p}/\omega_0 = 0.1$ and a Gaussian intensity distribution were assumed.

3.1 Axial force

The analytical approximation of the axial force is compared with the exact numerical integration as shown in Fig. 2. Fig. 2(a) shows the optical force in the axial direction as a function of the axial distance for various radial offsets. The maximum axial force occurs along the beam center axis when the radial offset is smaller than ω_0 while it is located off the beam center axis when the radial offset is larger than ω_0. This is due to the number of photons that strike the sphere. The number of photons is proportional to the intensity, i.e., the number of photons hitting the sphere is proportional to the intensity of the beam at the point where the sphere is located (Saleh and Teich 2007). Therefore, for a radial offset smaller than ω_0, the number of photons striking the sphere decreases as the sphere moves along the axial direction because the intensity decreases due to the broadening of the beam according to Eq. (4). On the contrary, for a radial offset larger than ω_0, the number of photons that hit

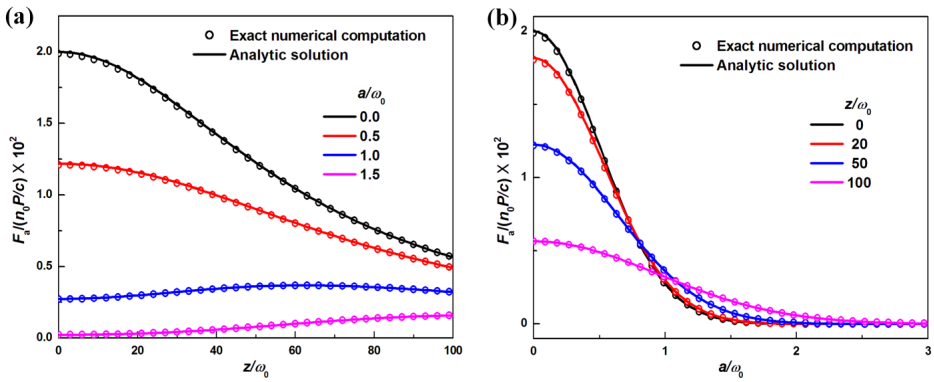

Fig. 2. Comparison between the analytical approximation and the exact numerical integration of the optical force in the axial direction: Axial force as a function of z-directional distance for various radial offsets (a) and axial force as a function of radial offset for various z-directional distance (b).

the sphere increases until the maximum value is reached, with the number then decreasing because the sphere or part of the sphere is located outside the beam ($1/e^2$ width) at z = 0 and enters the beam as the sphere moves along the axial direction. In the similar reason, the axial force monotonically decreases as shown in Fig. 2(b).

As indicated in Fig. 2 the derived analytic approximation agrees well with the exact numerical computation. The maximum error occurs at the minimum waist of the beam, i.e., $z = 0$ and $a = 0$. The maximum error due to the small sphere assumption on the axial force can be estimated by evaluating Eq. (6) at the minimum waist of the beam as follows,

$$\begin{aligned} F_{\mathrm{a,exact}}\big|_{z=0,\,a=0} &= \frac{8n_0P}{c}\left(\frac{r_\mathrm{p}}{\omega}\right)^2 \\ &\quad\times\left[\frac{\exp[-2(r_\mathrm{p}/\omega_0)^2]+2(r_\mathrm{p}/\omega_0)^2-1}{8(r_\mathrm{p}/\omega_0)^4}\right] \\ &= \frac{n_0P}{c}\left[\frac{4}{2!}\left(\frac{r_\mathrm{p}}{\omega_0}\right)^2-\frac{8}{3}\left(\frac{r_\mathrm{p}}{\omega_0}\right)^4+\cdots\right] \\ &= F_{\mathrm{a,analytic}}\big|_{z=0,\,a=0}+\frac{n_0P}{c}\sum_{k=1}^{\infty}\frac{(-1)^k2^{2k+1}}{(2k+1)!}\left(\frac{r_\mathrm{p}}{\omega_0}\right)^{2(k+1)}. \end{aligned} \tag{17}$$

Therefore, the maximum error due to the small sphere assumption is $\sim (r_\mathrm{p}/\omega_0)^4$ for $r_\mathrm{p} < \omega_0$.

3.2 Radial force

Figure 3 shows the comparison between analytical approximation and exact numerical integration of the optical force in the radial direction. Fig. 3(a) shows the radial force as a function of the axial distance for various radial offsets. Similar to the axial force, the maximum radial force occurs at the center axis of the beam for $a < \omega_0$, however, for $a > \omega_0$, the maximum radial force is located off the center axis of the beam. This is again due to the broadening of the beam width as the sphere moves along the axial direction. The radial force as a function of the radial offset for various axial distances is plotted in Fig. 3(b). Because the radial force originates from the variation in the intensity across the sphere, it is zero along the center axis of the beam. For a dielectric sphere, the radial force pulls the sphere to the center axis of the beam; however the radial force pushes away the perfectly reflecting sphere from the center axis of the beam. The location of the maximum radial force for a given axial distance can be determined by differentiating Eq. (14) with respect to the radial offset, i.e.,

$$\frac{\partial F_{\mathrm{r,anaytic}}}{\partial a}=0. \tag{18}$$

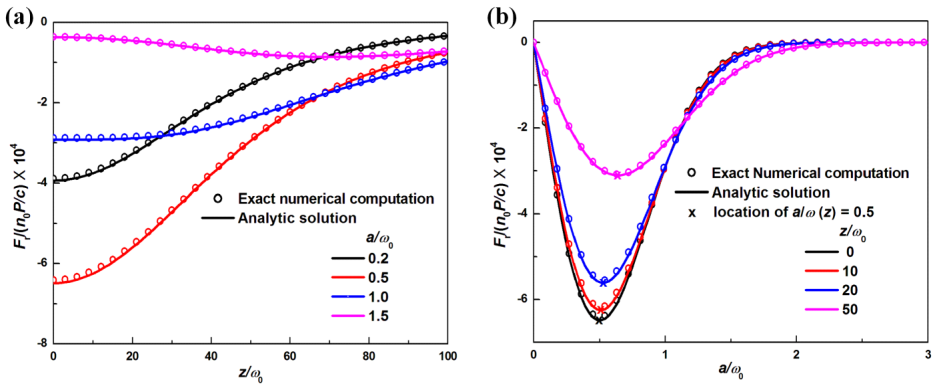

Fig. 3. Comparison between the analytical approximation and the exact numerical integration of the optical force in the radial direction: Radial force as a function of z-directional distance for various radial offsets (a) and radial force as a function of radial offset for various z-directional distance (b).

To evaluate Eq. (18), an asymptotic representation of the modified Bessel function of the first kind can be used (Watson, 1995),

$$\mathrm{I}_\nu(z) \sim \frac{1}{\Gamma(\nu+1)}\left(\frac{z}{2}\right)^\nu, \qquad 0 < |z| \ll \sqrt{\nu+1}\,. \tag{19}$$

From Eqs. (18) and (19), the location of the maximum radial force for the given axial distance can be obtained,

$$\frac{a}{\omega(z)} = \frac{1}{2}. \tag{20}$$

Equation (20) shows that the maximum radial force occurs when half of the sphere is located inside the beam ($1/e^2$ width). The location of the maximum variation in the intensity of the Gaussian beam coincides with Eq. (20).

According to Eq. (20), the maximum radial force can be written as,

$$F_{\mathrm{r,analytic}}\big|_{a/\omega=1/2} = -\frac{2n_0P}{c}\sqrt{\pi\frac{r_\mathrm{p}}{\omega}}\,e^{-1/2}\mathrm{I}_{5/2}\left(\frac{2r_\mathrm{p}}{\omega}\right). \tag{21}$$

The maximum error due to the small sphere assumption on the radial force can be estimated by evaluating Eq. (7) at $a/\omega(z) = 1/2$ as follows,

$$\begin{aligned} F_{\mathrm{a,exact}}\big|_{z=0,\,a=0} &= -\frac{8n_0P}{c}\left(\frac{r_\mathrm{p}}{\omega}\right)^2 e^{-1/2} \\ &\times \int_0^{\pi/2} \exp\left[-2\left(\frac{r_\mathrm{p}}{\omega}\sin\theta\right)^2\right] \mathrm{I}_1\left(2\frac{r_\mathrm{p}}{\omega}\sin\theta\right)\sin^2\theta\cos^2\theta\,\mathrm{d}\theta \\ &= -\frac{8n_0P}{c}\left(\frac{r_\mathrm{p}}{\omega}\right)^2 e^{-1/2}\left[\int_0^{\pi/2} \mathrm{I}_1\left(2\frac{r_\mathrm{p}}{\omega}\sin\theta\right)\sin^2\theta\cos^2\theta\,\mathrm{d}\theta\right. \\ &- 2\left(\frac{r_\mathrm{p}}{\omega}\right)^2 e^{-1/2}\int_0^{\pi/2} \mathrm{I}_1\left(2\frac{r_\mathrm{p}}{\omega}\sin\theta\right)\sin^4\theta\cos^2\theta\,\mathrm{d}\theta \\ &\left. - \frac{2^2}{2!}\left(\frac{r_\mathrm{p}}{\omega}\right)^4 e^{-1/2}\int_0^{\pi/2} \mathrm{I}_1\left(2\frac{r_\mathrm{p}}{\omega}\sin\theta\right)\sin^6\theta\cos^2\theta\,\mathrm{d}\theta + \cdots\right]. \end{aligned} \tag{22}$$

In the second line, a Taylor series expansion of the exponential function is used. The first term in the second line can be evaluated exactly using Eq. (11), and other terms can be approximated using (19) as follows,

$$\begin{aligned} &F_{\mathrm{r,exact}}\big|_{a/\omega=1/2} - F_{\mathrm{r,analytic}}\big|_{a/\omega=1/2} \\ &\sim \frac{8n_0P}{c}e^{-1/2}\sum_{k=1}^{\infty}(-1)^{k+1}\frac{2^k}{k!}\left(\frac{r_p}{\omega}\right)^{2k+3} B\left(k+2,\frac{3}{2}\right). \end{aligned} \tag{23}$$

where B is the beta function. Thus, the maximum error due to the small sphere assumption is $\sim (r_\mathrm{p}/\omega(z))^5$.

3.3 Optical forces at an arbitrary position

Compared to previous studies, one of the advantages of the analytic expression of the optical force derived in this study is that it can calculate both the axial and radial forces at an arbitrary position on the perfectly reflecting sphere. Figure 4 shows a three-dimensional optical force map of the perfectly reflecting sphere in the Gaussian intensity distribution. The radial force is two orders of magnitude smaller than the axial force. Based on Fig. 4, the perfectly reflecting sphere in the Gaussian beam moves parallel to the direction of beam propagation and tends to escape from the beam. These behaviors are similar to those of a dielectric sphere with a refractive index smaller than that of the surrounding medium.

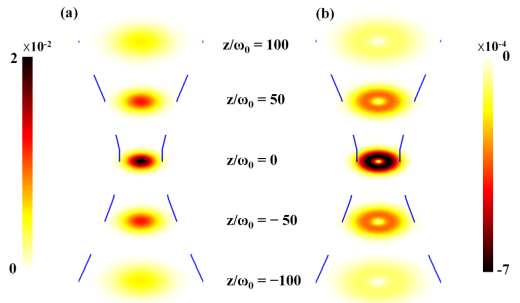

Fig. 4. Three-dimensional plotting of optical forces on a perfectly reflecting sphere in the Gaussian beam using the derived analytical expression: Axial force (a) and radial force (b). The optical forces are normalized by n_0P/c.

4. Conclusion

Closed-form analytic expressions of the optical force on a perfectly reflecting sphere in a ray-optics regime were derived and then compared to exact numerical calculations. The analytic expressions agreed well with the numerical calculations. The derived expressions provided a three-dimensional optical force map at an arbitrary position of the perfectly reflecting sphere. We also derived an analytical expression for the location of the maximum radial force and estimated the error due to the small sphere assumption by comparing with the exact numerical computation. The behavior of a perfectly reflecting sphere can be expected to be similar to a dielectric sphere with a refractive index smaller than that of the medium because the radial force pushes the sphere away from the center axis of the beam.

Acknowledgement

This work was supported by the Basic Research Fund (NK212E) from Korea Institute of Machinery and Materials.

References

Ashkin, A. (1970). Acceleration and trapping of particles by radiation pressure. Physical Review Letters, 24, 156-159.

Ashkin, A., and Dziedzic, J. M. (1989). Internal cell manipulation using infrared laser traps. Proceeding of the National Academy of Science U S A, 86, 7914-7918.

Chu, S., Bjorkholm, J. E., Ashkin, A., and Cable, A. (1986). Experimental observation of optically trapped atoms. Physiscal Review Letters, 57, 314-317.

Finer, J. T., Simmons, R. M., and Spudich, J. A. (1994). Single myosin molecule mechanics: Piconewton forces and nanometre steps. Nature, 368, 113-119.

Gauthier, R. C., and Wallace, S. (1995). Optical levitation of spheres: Analytical development and numerical computations of the force equations. Journal of the Optical Society of America B, 12, 1680-1686.

Gauthier, R. C. (1997). Optical trapping: A tool to assist optical machining. Optics & Laser Technology, 29, 389-399.

Hart, S. J., Terray, A., Arnold, J., and Leski, T. A. (2007). Sample concentration using optical chromatography. Optics Express, 15, 2724-2731.

Hebert, C. G., Terray, A., and Hart, S. J. (2011). Toward label-free optical fractionation of blood--optical force measurements of blood cells. Analytical Chemistry, 83, 5666-5672.

Kaneta, T., Ishidzu, Y., Mishima, N., and Imasaka, T. (1997). Theory of optical chromatography. Analytical Chemistry, 69, 2701-2710.

Kim, S. B., Kim, J. H., and Kim, S. S. (2006). Theoretical development of in situ optical particle separator: Cross-type optical chromatography. Applied Optics, 45, 6919-6924.

Kim, S. B., and Kim, S. S. (2006). Radiation forces on spheres in loosely focused gaussian beam: Ray-optics regime. Journal of the Optical Society of America B, 23, 897-903.

Kim, S. B., Yoon, S. Y., Sung, H. J., and Kim, S. S. (2008). Cross-type optical particle separation in a microchannel. Analytical Chemistry, 80, 2628-2630.

Koehler, D. R. (1997). Optical actuation of micro-mechanical components. Journal of the Optical Society of America B, 14, 2197-2203.

Kovac, J. R., and Voldman, J. (2007). Intuitive, image-based cell sorting using optofluidic cell sorting. Analytical Chemistry, 79, 9321-9330.

Lin, J., and Li, Y.-q. (2014). Optical trapping and rotation of airborne absorbing particles with a single focused laser beam. Applied Physics Letters, 104, 101909.

Lock, J. A. (2004). Calculation of the radiation trapping force for laser tweezers by use of generalized lorenz-mie theory. Ii. On-axis trapping force. Applied Optics, 43, 2545-2554.

Ozornek, M. H., Biefeld, P., and Jeyendran, R. S. (1998). Increased recovery of viable spermatozoa through oscillating centrifugation. Fertil Steril, 70, 712-714.

Paik, D. H., and Perkins, T. T. (2012). Single-molecule optical-trapping measurements with DNA anchored to an array of gold nanoposts. Methods in Molecular Biology, 875, 335-356.

Pan, Y.-L., Hill, S. C., and Coleman, M. (2012). Photophoretic trapping of absorbing particles in air and measurement of their single-particle raman spectra. Optics Express, 20, 5325-5334.

Saleh, B. E. A., and Teich, M. C. (2007). Fundamentals of photonics. Wiley Interscience, Hoboken, N.J.

Terray, A., Arnold, J., and Hart, S. J. (2005). Enhanced optical chromatography in a pdms microfluidic system. Optics Express, 13, 10406-10415.

Terray, A., Ladouceur, H. D., Hammond, M., and Hart, S. J. (2009). Numerical simulation of an optical chromatographic separator. Optics Express, 17, 2024-2032.

Terray, A., Hebert, C. G., and Hart, S. J. (2014). Optical chromatographic sample separation of hydrodynamically focused mixtures. Biomicrofluidics, 8, 064102.

Watson, G. N. (1995). A treatise on the theory of bessel functions. Cambridge University Press, Cambridge England ; New York.

Zhong, M. C., Wei, X. B., Zhou, J. H., Wang, Z. Q., and Li, Y. M. (2013). Trapping red blood cells in living animals using optical tweezers. Nature Commun, 4, 1768.